





## Article

# Northeast Asian Dust Transport: A Case Study of a Dust Storm Event from 28 March to 2 April 2012

Purevsuren Tsedendamba <sup>1,2</sup>, Jugder Dulam <sup>3</sup>, Kenji Baba <sup>2</sup> , Katsuro Hagiwara <sup>4</sup> , Jun Noda <sup>4</sup> , Kei Kawai <sup>5</sup>, Ganzorig Sumiya <sup>2</sup>, Christopher McCarthy <sup>6</sup>, Kenji Kai <sup>7</sup> and Buho Hoshino <sup>2,\*</sup> 

<sup>1</sup> National Agency for Meteorology and Environmental Monitoring, Ulaanbaatar 15160, Mongolia; pujee\_ts@yahoo.com (P.T.)

<sup>2</sup> Graduate School of Dairy Sciences, Rakuno Gakuen University, Ebetsu, Hokkaido 069-8501, Japan; kbaba@rakuno.ac.jp (K.B.); sgkanzorig@gmail.com (G.S.)

<sup>3</sup> Information and Research Institute of Meteorology, Hydrology and Environment, Mongolia National Agency for Meteorology and Environmental Monitoring, Ulaanbaatar 15160, Mongolia; jugderd@yahoo.com

<sup>4</sup> School of Veterinary Medicine, Rakuno Gakuen University, Ebetsu, Hokkaido 69-8501, Japan; k-hagi@rakuno.ac.jp (K.H.); jnoda@rakuno.ac.jp (J.N.)

<sup>5</sup> Graduate School of Environmental Studies, Nagoya University, Nagoya 464-8601, Japan; kawai.kei@e.mbox.nagoya-u.ac.jp

<sup>6</sup> Graduate School of Global Environmental Studies, Kyoto University, Kyoto 606-8501, Japan; mccarthy.ch@gmail.com

<sup>7</sup> College of Education, Ibaraki University, 2-1-1, Bunkyo, Mito 310-8512, Japan; kenji.kai.kk@vc.ibaraki.ac.jp

\* Correspondence: aosier@rakuno.ac.jp; Tel.: +81-011-388-4913

Received: 14 January 2019; Accepted: 2 February 2019; Published: 6 February 2019



**Abstract:** The distribution and transport of windblown dust that occurred in Northeast Asia from 28 March to 2 April 2012 was investigated. Data of particulate matter less than 10 micrometers (PM<sub>10</sub>) near the surface and light detection and ranging (LiDAR) measurements from the ground up to 18 km were used in the study. A severe dust event originated over southern Mongolia and northern China on 28 March 2012, and the widespread dust moved from the source area southeastward toward Japan over several days. Windblown dust reached Japan after two days from the originating area. LiDAR measurements of the vertical distribution of the dust were one to two km thick in the lower layer of the atmosphere, and increased with the increasing distance from the source area.

**Keywords:** LiDAR; dust storm; PM<sub>10</sub>; Northeast Asia; Gobi desert

## 1. Introduction

Dust storms are a common phenomenon in the desert regions of Northeast Asia, especially in the Gobi desert in southern Mongolia, northern China, and Taklamakan desert in northwest China [1–8]. Eastward and southeastward moving cyclones and the northwesterly wind often transport large amounts of fine dust particles to the eastern parts of China, the Korean Peninsula, and Japan [8]. Frequent Asian Dust vents in Japan during 2000–2002 followed severe dust outbreaks in East Asia [7].

Dust concentrations of PM<sub>10</sub> increase by at least double during severe dust events in comparison with normal atmospheric conditions [9,10]. PM<sub>10</sub> dust particles are the primary source of the yellow dust phenomenon that spreads across Northeast Asia [11]. Research has shown that Asian dust often reaches Korea [12–15], Taiwan [16–18], and Japan [7,8].

The transport of desert dust from Asia to the North Pacific atmosphere has been well documented [19–25]. The peak frequencies of dust storms occur from March to June and September [1]. Dust storms are classified as a type of natural disaster, which can affect ecosystems, human life,

and health [1,26–32]. Researchers have included the use of radiative transfer, chemical transport, weather forecasting, and global, numerical, and regional climate models [1,33–39] by using remote sensing [40–42] such as light detection and ranging (LiDAR) [43–45] and climatology to understand the dust transport linked with dust storm events in Mongolia and China [1,46,47].

Natsagdorj et al. (2003) have shown the number of dusty days has tripled from 1960 to 1999 [1]. In Mongolia, the number of days with dust storms is less than 10 days in the provinces of Altai, Khangai, Khuvsgul, and Khentii, more than 50 days in the Gobi desert region, and over 90 days in the southern part of Altai Gobi and far western regions of Mongolia [48,49].

The purpose of this study is to investigate the effects of long-distance transport from dust events occurring in Mongolia by cross-examining the elevated level of particulate matter in neighboring countries. With temporal variations and dust transport in Northeast Asia, we have used analyses of PM<sub>10</sub> concentration, back trajectory, and AD-Net LiDAR measurements at various locations during the period of 28 March to 2 April 2012.

## 2. Materials and Methods

### 2.1. Description of Dust Event

Atmospheric dust phenomena includes widespread dust suspension in the air and dust or sand raised by the wind, i.e., a dust/sandstorm (DSS) caused by turbulent winds raising large quantities of dust or sand into the air and severely reducing visibility, dust whirls or sand whirls, and occasionally funnel clouds. The WMO (World Meteorological Organization) protocol has been used; dust events are classified according to visibility into the four categories as described below [50]:

- Dust storm: strong winds lift large quantities of dust particles, reducing visibility to between 200 m and one kilometer.
- Drifting dust: dust is raised above the ground at eye level (<two meters) locally through strong winds. The horizontal visibility may be reduced up to 10 km.
- Floating dust: raised dust or sand at the time of observation, reducing visibility to one to 10 km.
- Dust devils or dust whirls: local, spatially limited columns of dust that neither travel far nor last long.

Dusty days are defined as the sum of days with dust storms and/or drifting dust. A strong surface wind was defined as a velocity exceeding 6.5 m/s (a constant threshold), which is the threshold of dust emission for many dust storm numerical models [1,7]. In this study, the DSS events are defined by the above-mentioned as the description of the dust events.

### 2.2. Surface Dust Concentration Data

We used the hourly averaged data of PM<sub>10</sub> concentration measured by the KOSA (Yellow Dust) Monitor of National Institute for Environmental Studies, Japan and National Agency for Meteorology, and Environmental Monitoring in Mongolia, China, and South Korea from 28 March to 2 April 2012 (Figure 1). In total, three Mongolian, nine Chinese, 11 Korean, and nine Japanese dust monitoring stations were used in the study (Figure 1). Exact locations are indicated in the following links [51–54].

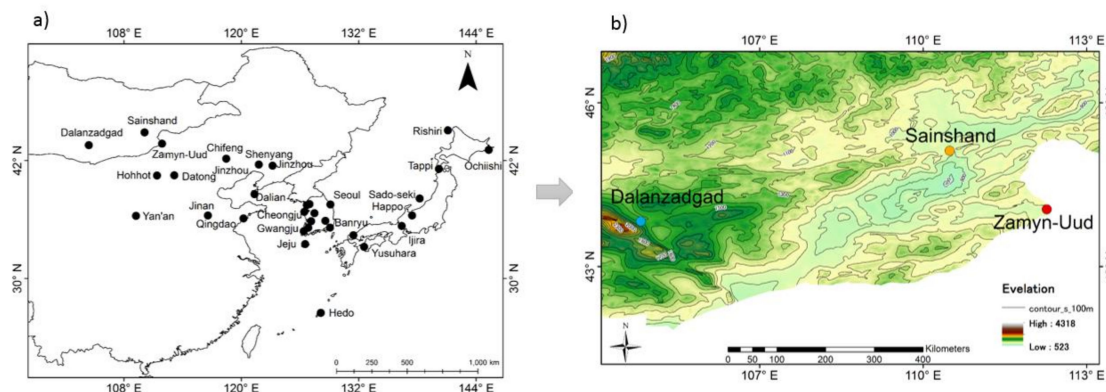


**Figure 1.** (a) Dust monitoring stations in Northeast Asia and (b) DEMs (digital elevation models) in the southern part Mongolia retrieval using NASA's Shuttle Radar Topography Mission (SRTM).

According to  $PM_{10}$ , data sites were obtained by KOSA monitors that measure light scattering, and are fitted with cyclone-type sizers (KOSA Monitor; TOA-DKK Co., Tokyo, Japan) [55].

The instrumentation of dust monitoring stations in Japan was sourced from the Ministry of the Environment in Japan.

The instrumentation of dust monitoring stations in China and Korea are available from the China National Environmental Monitoring Center and Korea Meteorological Administration, respectively.

### 2.3. LiDAR Monitoring Data for AD-Net (The Asian Dust and Aerosol Lidar Observation Network)

Data from Mie scattering LiDAR measurements at Sainshand ( $44.87^{\circ}\text{N}$ ,  $110.12^{\circ}\text{E}$ ), Seoul ( $37.57^{\circ}\text{N}$ ,  $126.98^{\circ}\text{E}$ ), and Hedo ( $26.87^{\circ}\text{N}$ ,  $128.25^{\circ}\text{E}$ ) were obtained from AD-Net (The Asian Dust and Aerosol Lidar Observation Network) [56,57] (Figure 2).

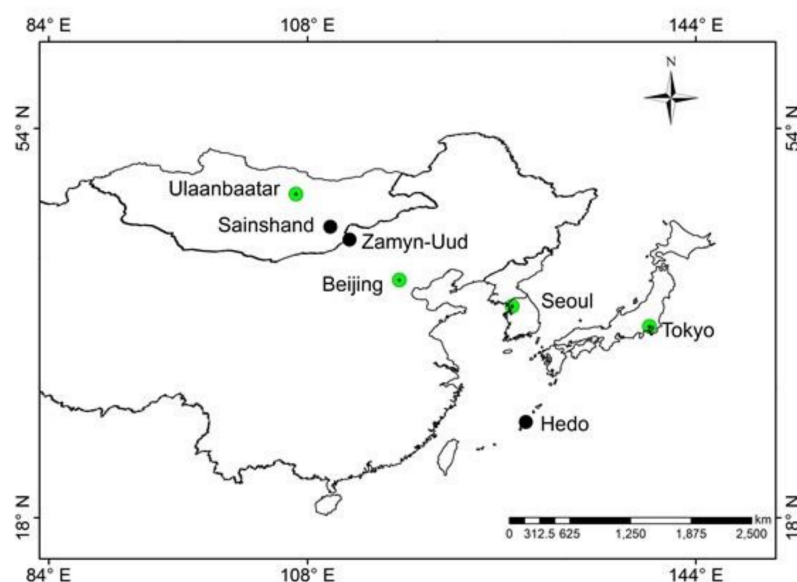


**Figure 2.** Locations of the AD-Net light detection and ranging (LiDAR) stations.

These LiDARs are operated by the National Institute for Environmental Studies (NIES), Japan and the National Agency for Meteorology and Environmental Monitoring (NAMEM), Mongolia. The AD-Net LiDAR measurements that are used in the study have two wavelengths (532 nm and 1064 nm), the pulse repetition rate is 10 Hz, and the pulse energy is 50 mJ. The polarization of backscatter light is measured at a wavelength of 532 nm. The main parameters of the Mie-scattering LiDARs are the depolarization ratio, attenuated backscattering coefficient, and extinction coefficient.

They are operated automatically, and the five-minute averaged LiDAR profiles are recorded every 15 min in the continuous observation mode [9,44,45,57].

#### 2.4. Meteorological Data

The hourly measurements of wind speed, visibility, and weather conditions from the daily surface and 500-hPa upper level charts produced by NAMEM were used.

Synoptic observations, including the wind speed, present weather and archive data (such as the number of dusty days and duration of dust storms) were obtained from three meteorological stations in Mongolia. The period during 1999 to 2016 was used for climatological analysis. ERA-Interim (ERA-Interim is a dataset, showing the results of a global climate reanalysis from 1979, continuously updated in real time) [58] data is used for wind at 10 m and pressure at sea surface level.

#### 2.5. Trajectory Method

We have used forward and backward trajectories of air mass movements using the reanalysis HYSPLIT (The Hybrid Single Particle Lagrangian Integrated Trajectory) Model from the NOAA (National Oceanic and Atmospheric Administration) [59] and archived meteorological data of NOAA.

### 3. Results and Discussion

#### 3.1. Number of Dusty Days, Its Trend, and PM<sub>10</sub> Concentration of Spring Season at Dalanzadgad, Sainshand, and Zamyn-Uud Stations, Mongolia

There is a clear annual variation in dust storm occurrence in Mongolia. In association with the movement of the mid-latitude cold frontal belt, the highest frequency (61%) of dust storms in Mongolia occurs in the spring, and the second maximum occurrence (22%) of dust storms occurred in the fall (October and November). The annual minimum frequency (7%) occurs in the summer, which is a period when low-pressure fields with small pressure gradients predominate across the country, and in the winter (10%), when cyclonic activity is weak and the air is largely stable [60]. We analyzed daily meteorological data for a period of 18 years between 1999–2016.

In previous study [10], the frequency and trends of sand/dust storms at the Dalanzadgad, Sainshand, and Zamyn-Uud stations between 1960–2012 have been described. In this study, we extended the data of sand/dust storms up to 2016.

The numbers of dusty days among the Gobi desert measurement stations: Dalanzadgad, Sainshand, and Zamyn-Uud, only the Zamyn-Uud station showed an increasing trend (Figure 3).

Dust storm frequency is higher during March and April than in the other months in Mongolia [1]. The monthly average concentration of PM<sub>10</sub> at Dalanzadgad, Sainshand, and Zamyn-Uud were higher in March and April between 2009–2017. The results are shown in Figure 4. This study is a continuation of previous studies (see [9,10]) and included the latest data of PM<sub>10</sub>. The higher dust storm frequencies and higher concentrations of PM<sub>10</sub> are most likely correlated. In 2013, from summer to winter, an instrument was disabled so that measurements of PM<sub>10</sub> concentration couldn't be collected. The monthly average concentrations of PM<sub>10</sub> varied from 36–46 µg/m<sup>3</sup> at Dalanzadgad in March and April between 2009–2017 except for in 2010, in which concentrations were as high as 60 µg/m<sup>3</sup>. According to climate data, precipitation was small, and for Dalanzadgad, 2010 was a drought year [60]. Conversely, the year 2017 was with higher precipitation and higher vegetation [60]. These climate conditions can influence the sand/dust storm frequencies at Dalanzadgad in those years.

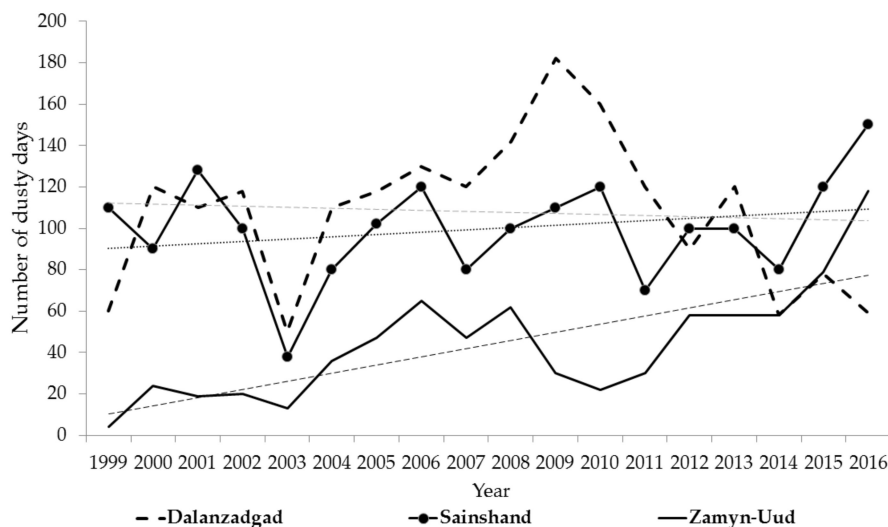


**Figure 3.** Number of dusty days at Dalanzadgad, Sainshand, and Zamyn-Uud between 1999–2016.

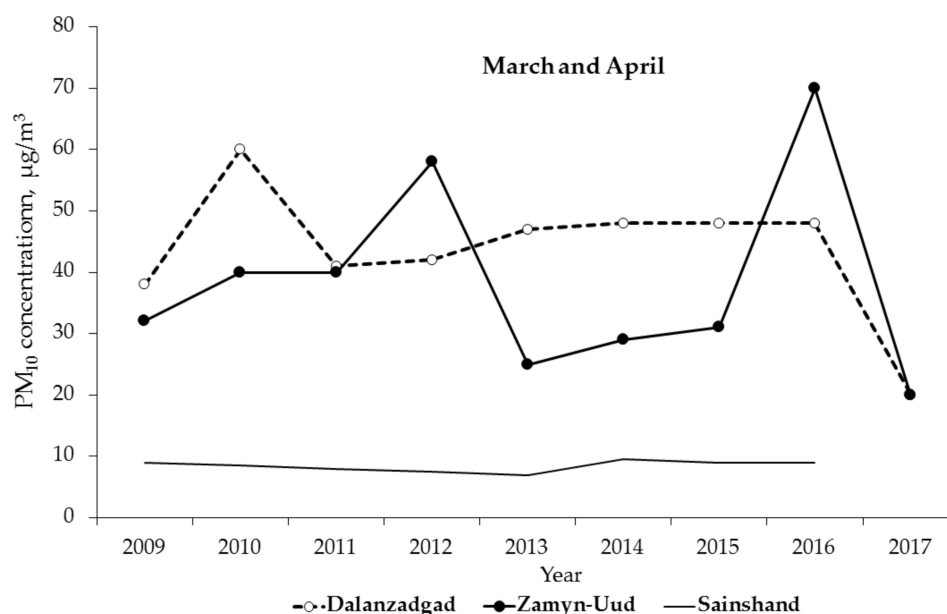


**Figure 4.** Monthly average datasets of PM<sub>10</sub> at Dalanzadgad, Sainshand, and Zamyn-Uud in March and April between 2009–2017.

The monthly average concentration of PM<sub>10</sub> at Zamyn-Uud in March to April was between 30–40 µg/m<sup>3</sup> in 2009–2011 and 25–30 µg/m<sup>3</sup> in 2013–2015, and as high as 60 µg/m<sup>3</sup> in 2012 and 71 µg/m<sup>3</sup> in 2016 (Figure 4). Climate data shows that precipitation was higher and vegetation growth was good around Zamyn-Uud in 2013–2015 and 2017. These climate conditions may influence the lower frequencies of sand/dust storms, causing low concentrations of PM<sub>10</sub>.

Concentrations were as low as 19–21 µg/m<sup>3</sup> at those two sites in 2017. The monthly average concentration of PM<sub>10</sub> at Sainshand was less than 10 µg/m<sup>3</sup> in March to April between 2009–2017.

### 3.2. Northeast Asian Dust Transport: A Case Study

#### 3.2.1. Meteorological Condition

A cyclonic circulation formed at sea level height; its wind speed increased and traveled from central Mongolia to east Mongolia on 28 March 2012 (Figure 5a). The low-pressure system moved



eastward with a high wind speed through northeast China, the Korean Peninsula, and Japan from 28 March to 2 April 2012 (Figure 5b,c).

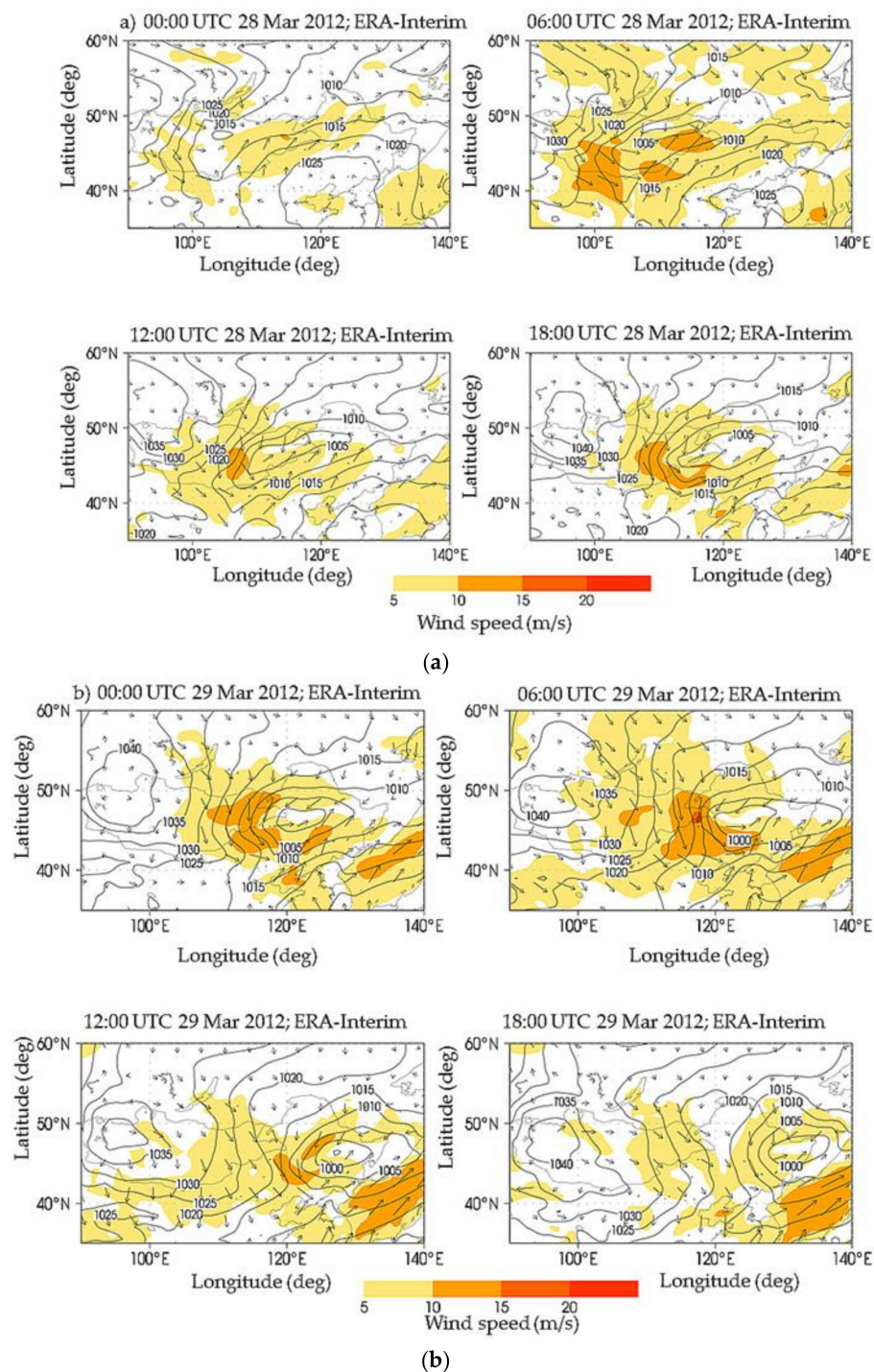


**Figure 5.** Sea level pressure (hPa) by contour and 10-m wind vectors using the ERA-Interim from 00:00 to 18:00 UTC on (a) 28 March 2012, (b) 29 March 2012, and (c) 30 March 2012 over Mongolia. The isobars interval is drawn in every five hPa and shading indicates wind speed (m/s).

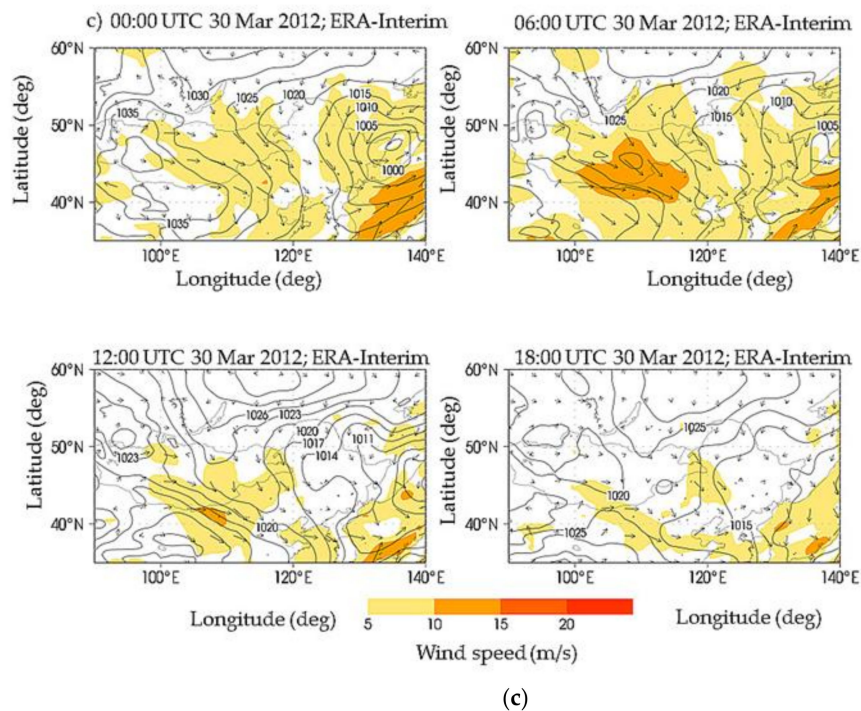


Figure 5. Cont.

Wind speeds increased in the dust source area, including the Gobi desert regions, in southern Mongolia and northern China due to the cyclonic pressure system. For example, daily maximum wind speeds varied at Dalanzadgad, Sainshand, and Zamyn-Uud stations from 10 m/s to 14 m/s. Maximum wind speed reached 14 m/s and the duration of the dust storm was around 12 h in Zamyn-Uud between 29–30 March 2012. Relative humidity was measured at between 7–12% at these sites during the dust storm period. High wind speeds in the Gobi desert regions produced a sufficient dust concentration of  $PM_{10}$  in the source areas.

Dust concentrations of  $PM_{10}$  increased by two times at the observation stations in Mongolia and China during 28–30 March, 2012. The reason is related to the atmospheric cold and warm fronts that passed through the Gobi desert areas of the two countries. Higher dust concentrations of  $PM_{10}$  in 28–30 March were in conjunction with the passage of the atmospheric cold and warm fronts, respectively.

### 3.2.2. Dust Concentrations of $PM_{10}$ in the Source Areas

**Mongolia:** The instrument measuring  $PM_{10}$  was disabled at Dalanzadgad during the peak dust storm period due to a cut in the power supply. Historically,  $PM_{10}$  concentrations are lower at Sainshand [9,10], which is a topic that should be explored in future studies. For these reasons, these two sites could not provide reliable data on  $PM_{10}$ . However,  $PM_{10}$  dust concentrations at Zamyn-Uud showed the dust event perfectly. Hourly mean dust concentrations of  $PM_{10}$  were as high as  $404 \mu\text{g}/\text{m}^3$  at Zamyn-Uud during the dust event period (Figure 6). Dust concentrations of  $PM_{10}$  at Zamyn-Uud reached the threshold values of the onset of dust events [10].

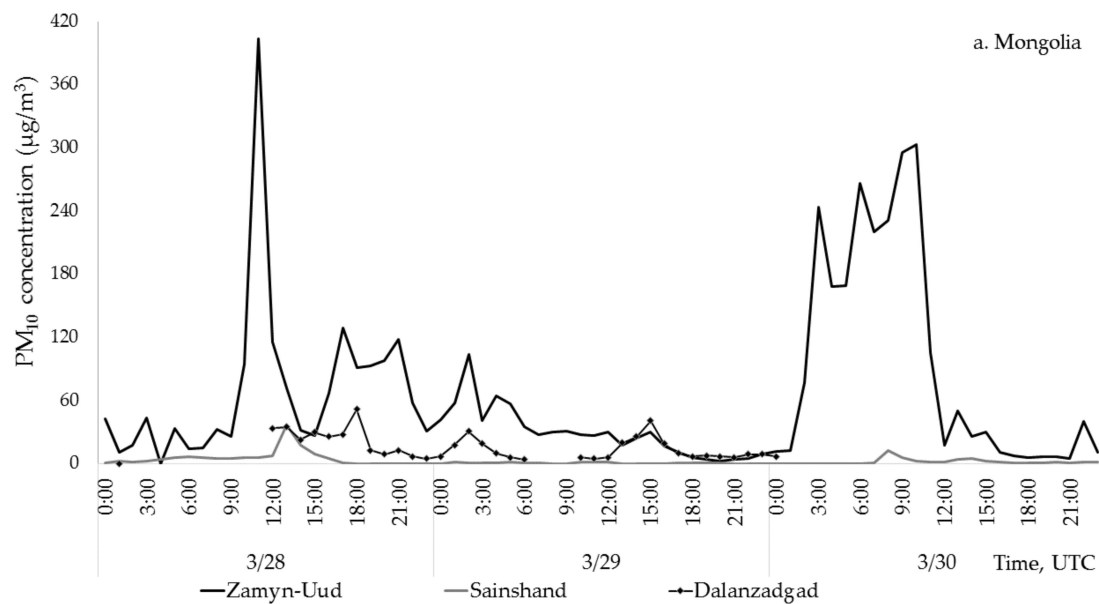


**Figure 6.** Time series variations of dust concentration of  $PM_{10}$  at stations in Mongolia.

China: Hourly mean dust concentrations of  $PM_{10}$  were higher than usual,  $999 \mu\text{g}/\text{m}^3$ , at Hohhot and  $1387 \mu\text{g}/\text{m}^3$  at Chifeng between 28–29 March 2012, while concentrations at Hohhot measured  $1724 \mu\text{g}/\text{m}^3$  on 30 March and around  $599 \mu\text{g}/\text{m}^3$  in Qingdao and Dalian on 31 March, respectively (Figure 7). Concentrations fluctuated under  $400 \mu\text{g}/\text{m}^3$  at the other stations during the study period.

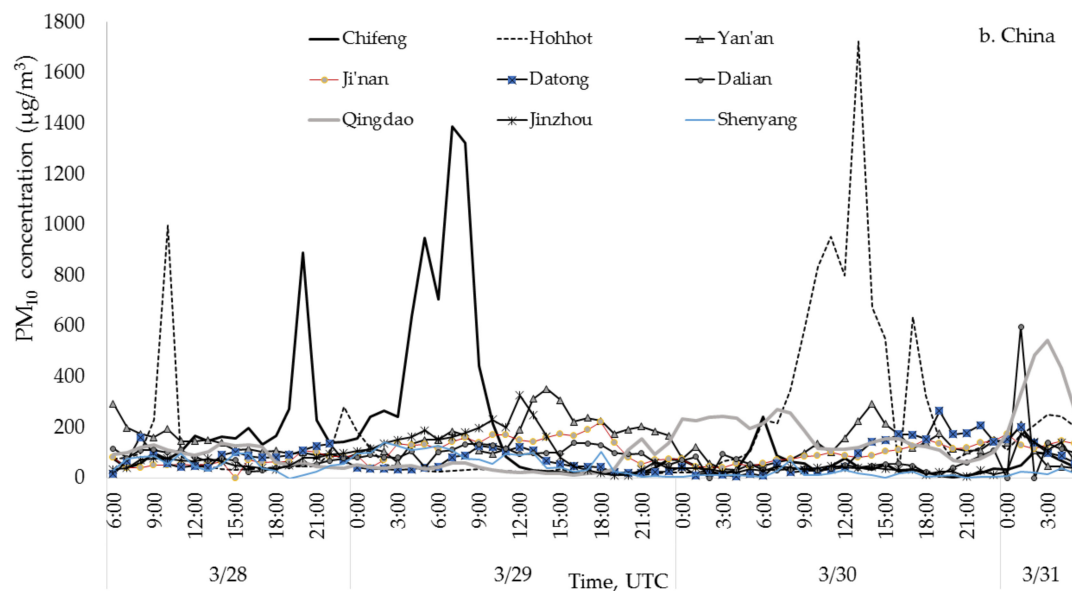


**Figure 7.** Time series variations of dust concentration of  $PM_{10}$  at stations in China.

### 3.2.3. Dust Concentrations of $PM_{10}$ in Downwind Areas

South Korea: Maximum values of hourly mean dust concentrations of  $PM_{10}$  were between  $225\text{--}266 \mu\text{g}/\text{m}^3$  in Jeju, Incheon, and Cheongju on 31 March and varied from  $147$  to  $182 \mu\text{g}/\text{m}^3$  at the other stations between 31 March and 2 April 2012 (Figure 8).



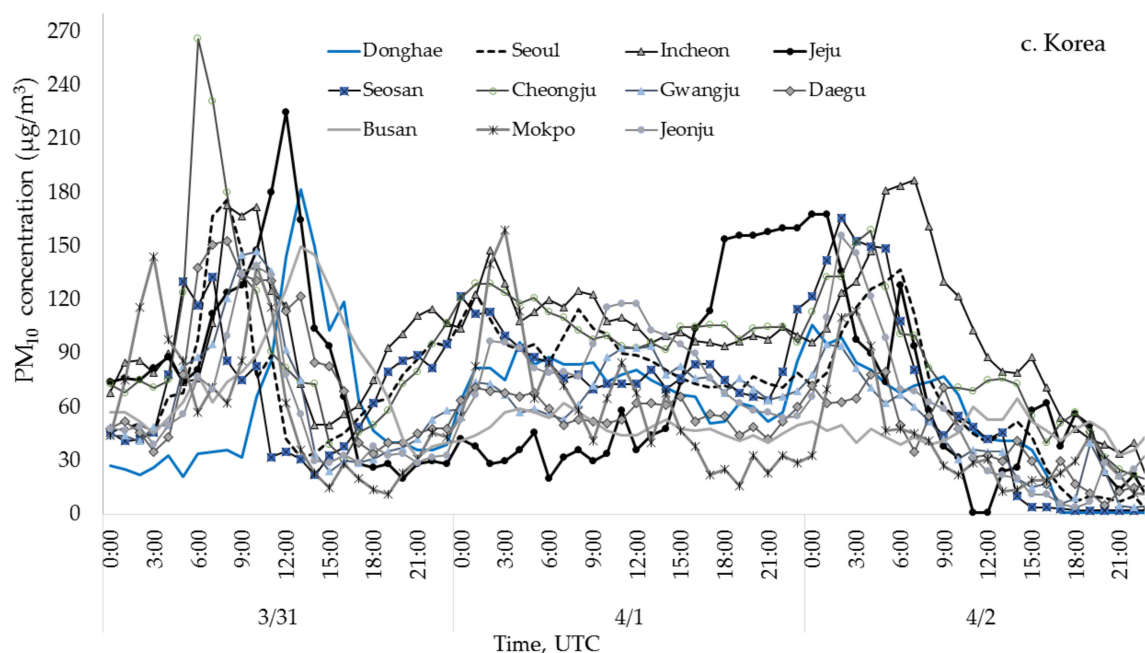


**Figure 8.** Time series variations of dust concentration of PM<sub>10</sub> at stations in Korea.

Japan: Dust concentrations of PM<sub>10</sub> were higher at Hedo station (compared to all of the other stations), which is located on the north side of the island of Okinawa, Japan. Hourly mean dust concentrations of PM<sub>10</sub> were higher, between 104–207 µg/m<sup>3</sup>, at Hedo station from 31 March to 1 April 2012 (Figure 9). Concentrations increased at Banryu station in Yamaguchi Prefecture in northwest Japan and in Yusuvara station in Ehime Prefecture, Japan during the same days. Hourly mean dust concentrations of PM<sub>10</sub> increased slightly to 100 µg/m<sup>3</sup> at the other stations in Japan on 2 April (Figure 9). Dust concentrations of PM<sub>10</sub> near the surface were higher in the source area during the dust storm period and decreased in the downwind areas.

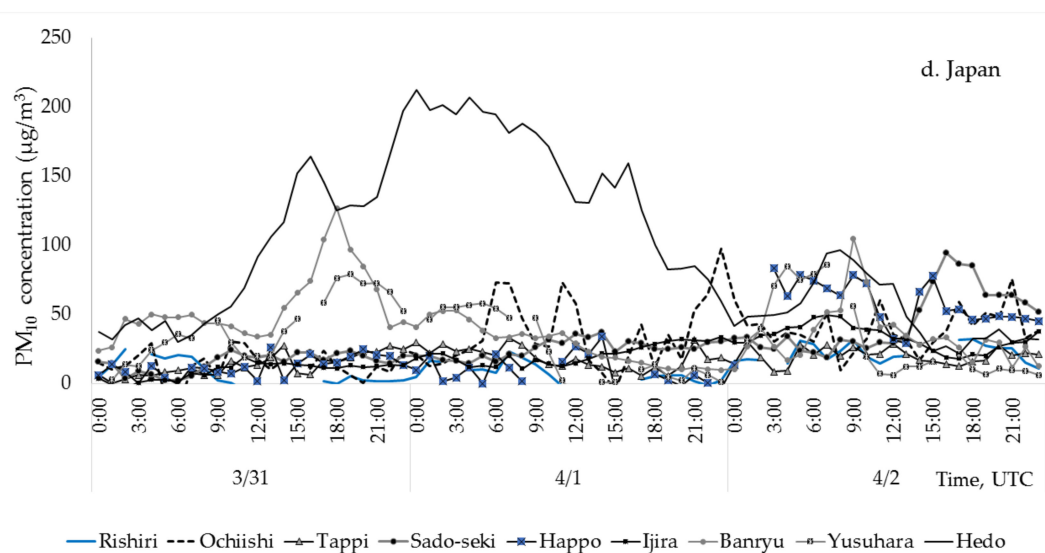


**Figure 9.** Time series variations of dust concentration of PM<sub>10</sub> at stations in Japan.

### 3.2.4. Vertical Distribution of Dust by LiDAR Measurements and Transport Trajectories

Dust vertical spread was measured by LiDAR in Mongolia, Korea and Japan during the dust storm period. Figure 10 shows time–height indications of extinction coefficients of non-spherical aerosols (mostly mineral dust) and spherical aerosol (mostly anthropogenic particles) derived from LiDAR

measurements [61,62]. LiDAR measurements show that the soil dust (upper panel) that was recorded at Sainshand between March 28–29 (Figure 10a) and at Seoul and Hedo stations from 10 March to 1 April 2012 (see Figure 10a–c).

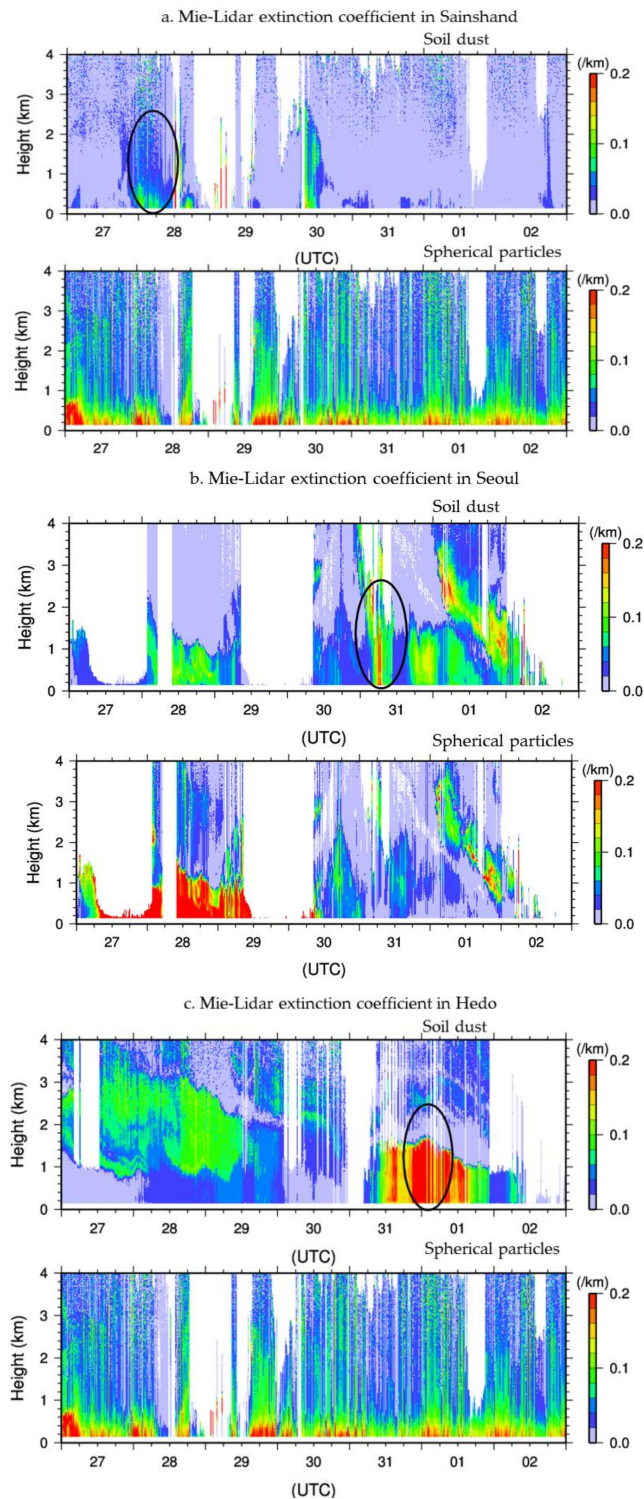


**Figure 10.** The Mie LiDAR extinction coefficients of non-spherical aerosol (dust) and spherical aerosol in (a) Sainshand, (b) Seoul, and (c) Hedo from 28 March to 2 April 2012 (Note: Time (UTC) in the horizontal axis and height in the vertical axis. The black circles indicate suspected dust observation).

The heights of dust vertical spread were around 0.7 km in Sainshand, between 28–29 March 2012 (see Figure 10a) and around 1.2 km in Seoul, Korea (see Figure 10b) and around 1.5 km around Hedo (Figure 10c), Japan between 31 March and 2 April, respectively.

In this study, we have aimed to understand the natural soil dust events. However, anthropogenic dust or air pollution can be detected by LiDAR observations, which may need to be differentiated. Anthropogenic dust or air pollution (spherical particles) was detected by LiDAR at up to 800 m at the Sainshand and Hedo stations every day from 27 March to 2 April 2012 (Figure 10a), while it was detected up to 1.5 km high at Seoul station from 27 March to 30 March 2012 (Figure 10b).

LiDAR measurements showed that the vertical diffusion of dust in the atmosphere was lower in the source area during the dust storm period and increased with distance in the downwind areas. PM<sub>10</sub> concentration sources originated in Mongolia, which we confirmed with the NOAA HYSPLIT model.

### 3.2.5. Dust Transport by Air Mass Trajectories

Forward and backward trajectories from the NOAA HYSPLIT model were used for air mass movements in Northeast Asia during the dust storm period from 29 March to 2 April 2012 (Figure 11). To create the trajectories, we set the geographical coordinates of four stations in Northeast Asia including Zamyn-Uud, Hohhot, Seoul, and Hedo. A forward trajectory from Zamyn-uud, Mongolia ending at 00:00 UTC on 30 March and backward trajectories from Hohhot ending at 00:00 UTC on 31 March and Seoul and Hedo ending at 00:00 UTC on 1 April 2012 were created at heights of 1500 m, 2000 m, and 2500 m, respectively (Figure 11).

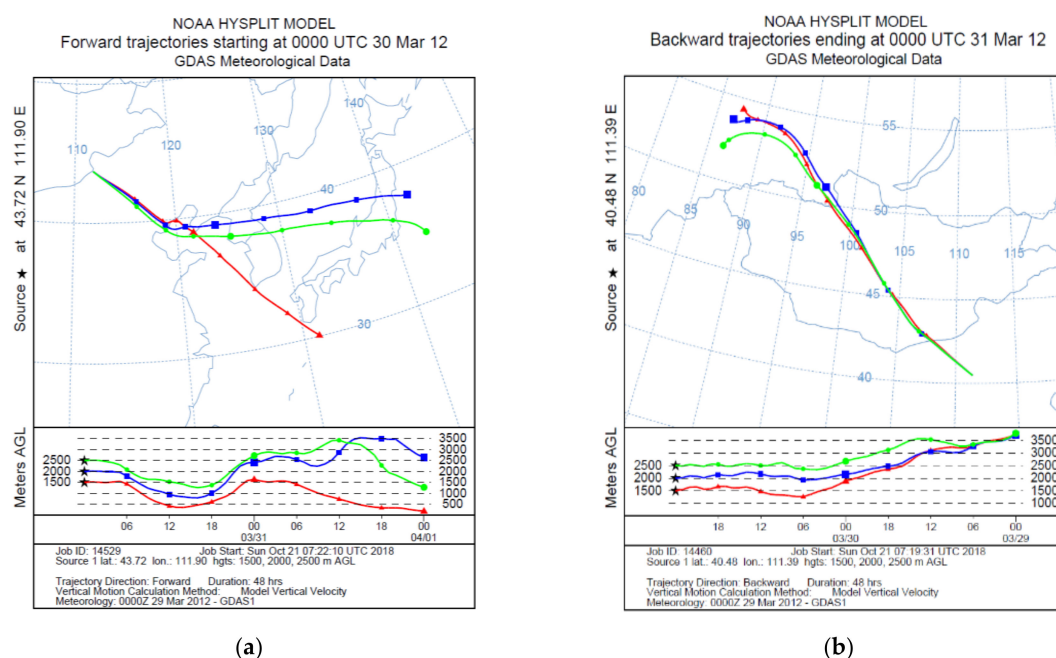


**Figure 11.** Forward and backward air mass trajectories using the NOAA HYSPLIT model: (a) forward from Zamyn-Uud, Mongolia, (b) backward from Hohhot, China, (c) backward from Seoul, Korea, and (d) backward from Hedo, Japan.

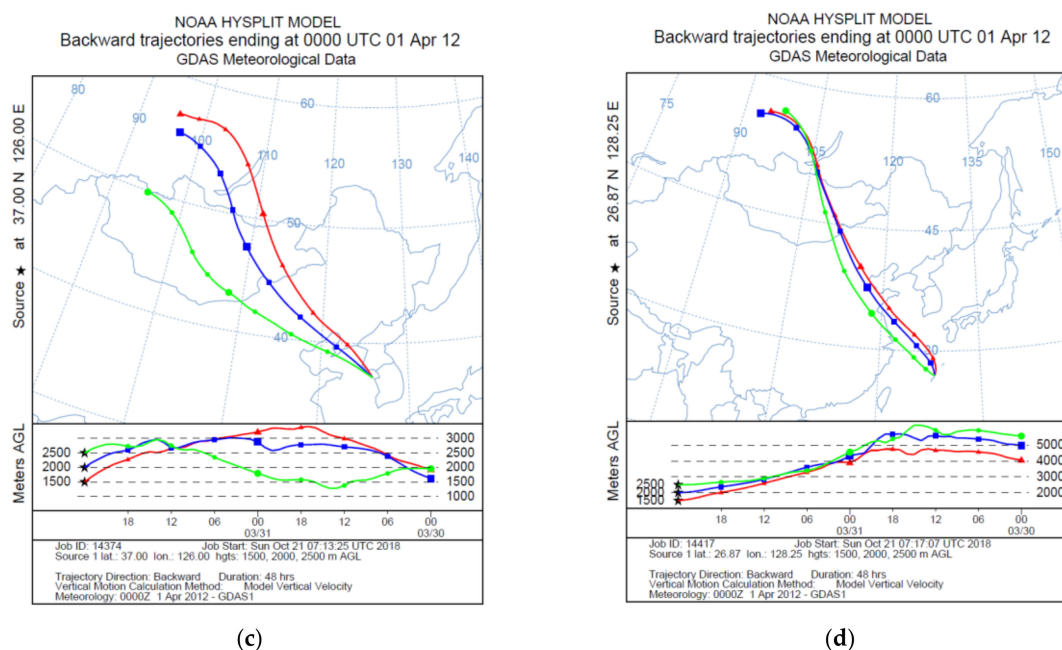


Figure 11. Cont.

The air mass movements at these heights mainly confirm the far transfer of air mass impurities at regional and global scales [63].

In addition, the average heights of dust layers during the dust storm event were around 2.2 km at Zamyn-Uud and 2.0 km at Sainshand [64]. Trajectories had a window of 48 h.

The episode of forward trajectories of air mass movement from Zamyn-Uud, Mongolia (30 March 2012) is presented (Figure 11a) for illustration. Apparently, from Figure 11, air mass from the Mongolian Gobi desert passed over the eastern territories of China, the Korean Peninsula, and Japan.

The results of the calculation of air mass backward trajectories show air mass transported from the Gobi desert areas in southern Mongolia and in northern China to the eastern parts of China, the Korea peninsula, and Japan (Figure 11b–d). These trajectories of air mass confirmed that dust was transported from the source areas downwind through Northeast Asia.

### 3.2.6. Discussion

The NOAA HYSPLIT model was used to analyze the air mass movements that moved from Russia to Mongolia on 30 March, 2012 and then traveled through southern to eastern Mongolia, eastern China, and the Korean Peninsula on 1 April, 2012 and then through Japan to the Pacific Ocean (Figure 11).

The Sainshand station between 28–29 March, 2012; Seoul station on 31 March, 2012 and the Hedo station on 1 April, 2012 all had dust movement that were observed by LiDAR measurements. We analyzed each station's dust transportation by NOAA HYSPLIT.

The Hedo station's  $PM_{10}$  concentration was the highest value to come from Mongolia, as shown in Figure 11a. Along with the Hedo station's backward trajectory,  $PM_{10}$  concentrations were observed higher than the  $150 \mu\text{g}/\text{m}^3$  value at the Hohhot and Qingdao stations.

Although there were observations of some fluctuations of dust concentration at Datong station, which is situated 150 km from Hohhot, and Yanan station which is located 513 km from Hohhot, those values only slightly exceeded the  $150 \mu\text{g}/\text{m}^3$  standard value.

At the Seoul station, dust movement was observed higher than the  $100 \mu\text{g}/\text{m}^3$  standard value from the northwest as it moved through the Chifeng station.

The highest dust fluctuation has been observed at the Incheon station, which is located 33 km from the Seoul station. Also, a low increase of dust concentration,  $90 \mu\text{g}/\text{m}^3$  of the standard value,



was observed at the Banryu station, which is located 544 km from the Seoul station. That increase was slightly more than the country standard value. Dust movements were observed at Tappi station, which is located 1273 km from the Seoul station, and at Sado-Seki station, which is situated 1003 km from the Seoul station, respectively; however, these values did not differ from regular meanings.

The PM<sub>10</sub> concentration maximum value in Mongolia was 404 µg/m<sup>3</sup> on 28 March 2012, while 999 µg/m<sup>3</sup> was observed in China, respectively. In Korea, the PM<sub>10</sub> concentration maximum value was observed on 30–31 March, 2012 as 266 µg/m<sup>3</sup>. Lastly the Mongolian Gobi area's dust storm was active as it moved to Japan on 1 April, 2012 with a PM<sub>10</sub> concentration maximum value of 212 µg/m<sup>3</sup>.

#### 4. Conclusions

An Asian dust event occurring from 28 March to 2 April 2012 was analyzed by ground observations of PM<sub>10</sub>, dust vertical spread by AD-Net LiDAR measurements, and dust transport by air mass trajectories using the NOAA HYSPLIT model. The main results are summarized as follows:

1. The climatological data of dusty days showed that only the number of dusty days at Zamyn-Uud, Mongolia had an increasing trend.
2. A low-pressure system and its cold front resulted in strong winds that transported dust from the source area across Northeast Asia at the end of March and the beginning of April 2012. The dust storm also created an increase in PM<sub>10</sub> particles in the dust source area, as well as in the downwind areas. Dust concentrations of PM<sub>10</sub> near the surface were higher in the source areas of the Gobi desert in Mongolia and China, and less in the downwind areas during transport, such as in Korea and Japan.
3. LiDAR measurements showed that dust vertical diffusion in the atmosphere was lower in the source area during the dust storm period, and increased in the downwind areas, especially when transported across far distances.
4. The trajectories of air mass confirmed that dust can be transported from the dust source areas in Mongolia and China to the Korean Peninsula and Japan.

**Author Contributions:** P.T.; J.D.; J.N.; G.S.; C.M. and B.H. analyzed the data and wrote the draft of the manuscript and designed the study. K.K.; P.T.; K.H.; K.B. and K.K. participated in the field measurements and participated in the LiDAR and meteorological images analysis.

**Funding:** This work was supported by JSPS KAKENHI Grant Numbers (JP)26281003; (JP)16H02703 and (JP)18H03608 and the MEXT Supported Program for the Strategic Research Foundation (S1391001) at Rakuno Gakuen University. We would like to thank Dr. Atsushi Shimizu, B. Alsaadeh for giving some kind advice about this paper. Also, LiDAR data was provided by AD-Net, we deeply appreciate it here.

**Conflicts of Interest:** The authors declare no conflict of interest.

#### References

1. Natsagdorj, L.; Jugder, D.; Chung, Y.S. Analysis of dust storms observed in Mongolia during 1937–1999. *Atmos. Environ.* **2003**, *37*, 1401–1411. [\[CrossRef\]](#)
2. Xuan, J.; Sokolik, I.N.; Hao, J.; Guo, F.; Mao, H.; Yang, G. Identification and characterization of sources of atmospheric mineral dust in East Asia. *J. Atmos. Environ.* **2004**, *38*, 6239–6252. [\[CrossRef\]](#)
3. Hoshino, B.; Demura, Y.; Sofue, Y.; Kai, K.; Purevsuren, T.; Noda, J. Estimates of ground surface characteristics for outbreaks of the Asian Dust Storms in the sources region. *ProScience* **2016**, *3*, 21–30.
4. Zhou, Z.J.; Zhang, G.C. Typical severe dust storms in northern China during 1954–2002. *Chin. Sci. Bull.* **2003**, *48*, 2366–2370. [\[CrossRef\]](#)
5. Chun, Y.; Boo, K.; Kim, J.; Park, S.; Lee, M. Synopsis, transport, and physical characteristics of Asian dust in Korea. *J. Geophys. Res.* **2001**, *106*, 18461–18469. [\[CrossRef\]](#)
6. Qian, W.H.; Quan, L.S.; Shi, S.Y. Variations of the dust storm in China and its climatic control. *J. Clim.* **2002**, *15*, 1216–1229. [\[CrossRef\]](#)



7. Kurosaki, Y.; Mikami, M. Recent frequent dust events and their relation to surface wind in East Asia. *Geophys. Res. Lett.* **2003**, *30*, 1736. [[CrossRef](#)]
8. Shao, Y.; Wang, J.A. Climatology of Northeast Asian dust events. *Meteorol. Z.* **2003**, *12*, 187–196. [[CrossRef](#)]
9. Jugder, D.; Shinoda, M.; Sugimoto, N.; Matsui, I.; Nishikawa, M.; Park, S.U.; Chun, Y.S.; Park, M.S. Spatial and temporal variations of dust concentrations in the Gobi Desert of Mongolia. *J. Glob. Planet. Chang.* **2011**, *78*, 14–22. [[CrossRef](#)]
10. Jugder, D.; Shinoda, M.; Kimura, R.; Batbold, A.; Amarjargal, D. Quantitative analysis on windblown dust concentrations of PM<sub>10</sub> (PM<sub>2.5</sub>) during dust events in Mongolia. *Aeolian Res.* **2014**, *14*, 3–13. [[CrossRef](#)]
11. Shao, Y. *Physics and Modelling of Wind Erosion*; Springer Science & Business Media: New York, NY, USA, 2008.
12. Lim, H.; Choi, G. Seasonal and interannual variability of Asian desert aerosols from Nimbus 7/TOMS Data. *IEEE Trans. Geosci. Remote Sens.* **2002**, *5*, 2945–2947. [[CrossRef](#)]
13. Chung, Y.S.; Yoon, M. B On the occurrence of yellow sand and atmospheric loading. *Atmos. Environ.* **1996**, *30*, 2387–2397.
14. Kim, J. Transport routes and source regions of Asian dust observed in Korea during the past 40 years (1965–2004). *Atmos. Environ.* **2008**, *42*, e4778–e4789. [[CrossRef](#)]
15. Uno, I.; Osada, K.; Yumimoto, K.; Wang, Z.; Itahashi, S.; Tahashi, S.; Pan, X.; Hara, Y.; Yamamoto, S.; Nishizawa, T. Importance of long-range nitrate transport based on long-term observation and modeling of dust and pollutants over East Asia. *Atmos. Chem. Phys.* **2017**, *17*, 14181–14197. [[CrossRef](#)]
16. Tsai, F.J.; Fang, Y.S.; Huang, S.J. Case study of Asian dust event on March 19–25, 2010 and its impact on the marginal sea of China. *J. Mar. Sci. Technol.* **2013**, *21*, 353–360.
17. Lin, C.Y.; Liu, S.C.; Chou, C.C.-K.; Liu, T.H.; Lee, C.-T.; Yuan, C.-S.; Shiu, C.-J.; Young, C.L. Long-range transport of Asian dust and air pollutants to Taiwan. *Terr. Atmos. Ocean. Sci.* **2004**, *15*, 759–784. [[CrossRef](#)]
18. Liu, G.R.; Lin, T.H. Application of geostationary satellite observations for monitoring dust storms of Asia. *Terr. Atmos. Ocean. Sci.* **2004**, *15*, 825–837. [[CrossRef](#)]
19. Shaw, G.E. Transport of Asian desert aerosol to the Hawaiian Islands. *J. Appl. Meteorol.* **1980**, *19*, 1254–1259. [[CrossRef](#)]
20. Parrington, J.R.; Zoller, W.H.; Aras, N.K. Asian dust: Seasonal transport to the Hawaiian Islands. *Science* **1983**, *20*, 195–197. [[CrossRef](#)]
21. Uematsu, M.; Duce, R.A.; Prospero, J.M.; Chen, L.; Merrill, J.T.; McDonald, R.L. Transport of mineral aerosol from Asia over the North Pacific Ocean. *J. Geophys. Res.* **1983**, *88*, 5343–5352. [[CrossRef](#)]
22. Merrill, J.T.; Uematsu, M.; Bleck, R. Meteorological analysis of long range transport of mineral aerosols over the North Pacific. *J. Geophys. Res.* **1989**, *94*, 8584–8598. [[CrossRef](#)]
23. Bodhaine, B.A. Aerosol absorption measurements at Barrow, Mauna Loa and the South Pole. *J. Geophys. Res.* **1995**, *100*, 8967–8975. [[CrossRef](#)]
24. Tan, S.; Li, J.; Che, H.; Chen, B.; Wang, H. Transport of East Asian dust storms to the marginal seas of China and the southern North Pacific in spring 2010. *Atmos. Environ.* **2017**, *148*, 316–328. [[CrossRef](#)]
25. Uno, I.; Eguchi, K.; Yumimoto, K.; Takemura, T.; Shimizu, A.; Uematsu, M.; Liu, Z.; Wang, Z.; Hara, Y.; Sugimoto, N. Asian dust transported one full circuit around the globe. *Nat. Geosci.* **2009**, *2*, 557–560. [[CrossRef](#)]
26. Kwon, H.J.; Cho, S.H.; Chun, Y.; Lagarde, F.; Pershagen, G. Effects of the Asian dust events on daily mortality in Seoul, Korea. *Environ. Res.* **2002**, *90*, 1–5. [[CrossRef](#)] [[PubMed](#)]
27. Griffin, D.W.; Garrison, V.H.; Herman, J.R.; Shinn, E.A. African desert dust in the Caribbean atmosphere. *Microbiol. Public Health Aerobiol.* **2001**, *17*, 203–213.
28. Garrison, V.H.; Shinn, E.A.; Foreman, W.T.; Griffin, D.W.; Holmas, C.W.; Kellogg, C.A.; Majewski, M.S.; Richardsan, L.L.; Ritchie, K.B.; Swith, G.W. African and Asian dust: From desert soils to coral reefs. *BioScience* **2003**, *53*, 469–480. [[CrossRef](#)]
29. Kellogg, C.A.; Griffin, D.W.; Garrison, V.H.; Peak, H.K.; Royal, N.; Smith, R.M.; Shinn, E.A. Characterization of aerosolized bacteria and fungi from desert dust events in Mali, West Africa. *Aerobiologia* **2004**, *20*, 99–110. [[CrossRef](#)]
30. Griffin, D.W. Atmospheric movement of microorganisms in clouds of desert dust and implications for human health. *Clin. Microbiol. Rev.* **2007**, *20*, 459–477. [[CrossRef](#)]

31. Higashi, T.; Kambayashi, Y.; Ohkura, N.; Fujimura, M.; Nakanishi, S.; Yoshizaki, T.; Saijoh, K.; Hayakawa, K.; Kobayashi, F.; Michigami, Y.; et al. Exacerbation of daily cough and allergic symptoms in adult patients with chronic cough by Asian dust: A hospital-based study in Kanazawa. *Atmos. Environ.* **2014**, *97*, 537–543. [[CrossRef](#)]
32. Taylor, D.A. Dust in the wind. *Environ. Health Perspect.* **2002**, *110*, A80–A87. [[CrossRef](#)]
33. Uno, I.; Carmichael, G.R.; Streets, D.G.; Tang, Y.; Yienger, J.J.; Satake, S.; Wang, Z.; Woo, J.H.; Guttikunda, S.; Uematsu, M.; et al. Regional chemical weather forecasting system CFORS: Model descriptions and analysis of surface observations at Japanese island stations during the ACE-Asia experiment. *J. Geophys. Res. Atmos.* **2003**, *108*. [[CrossRef](#)]
34. Liu, M.; Westphal, D.L.; Wang, S.; Shimizu, A.; Sugimoto, N.; Zhou, J.; Chen, Y. A high-resolution numerical study of the Asian dust storms of April. *J. Geophys. Res.* **2001**, *108*, 8653. [[CrossRef](#)]
35. Luo, C.; Mahowald, N.M.; Corral, J.D. Sensitivity study of meteorological parameters on mineral aerosol mobilization transport, and distribution. *J. Geophys. Res.* **2003**, *108*, 4447. [[CrossRef](#)]
36. Zender, C.S.; Bian, H.; Newman, D. Mineral Dust En-102 JOURNAL OF CLIMATE VOLUME 19 training and Deposition (DEAD) model: Description and 1990s dust climatology. *J. Geophys. Res.* **2003**, *108*, 4416. [[CrossRef](#)]
37. Igarashi, Y.; Fujiwara, H.; Jugder, D. Change of the Asian dust source region deduced from the composition of anthropogenic radionuclides in surface soil in Mongolia. *J. Atmos. Chem. Phys.* **2011**, *11*, 7069–7080. [[CrossRef](#)]
38. Ishizuka, M.; Mikami, M.; Yamada, Y.; Kimura, R.; Kurosaki, Y.; Jugder, D.; Gantsetseg, B.; Cheng, Y.; Shinoda, M. Does ground surface soil aggregation affect transition of the wind speed threshold for saltation and dust emission. *SOLA* **2012**, *8*, 129–132. [[CrossRef](#)]
39. Sun, H.; Pan, Z.T.; Liu, X.D. Numerical simulation of spatial-temporal distribution of dust aerosol and its direct radiative effects on East Asian climate. *J. Geophys. Res.* **2012**, *117*. [[CrossRef](#)]
40. Husar, R.B.; Tratt, D.M.; Schichtel, B.A.; Falke, S.R.; Li, F.; Jaffe, D.; Gasso, S.; Gill, T.; Laulainen, N.S.; Lu, F.; et al. Asian dust events of April 1998. *J. Geophys. Res.* **2001**, *106*, 18317–18330. [[CrossRef](#)]
41. Prospero, J.M.; Ginoux, P.; Torres, O.; Nicholson, S.E.; Gill, T.E. Environmental Characterization of Global Sources of Atmospheric Soil Dust Identified with the NIMBUS 7 Total Ozone Mapping Spectrometer (TOMS) Absorbing Aerosol Product. *Rev. Geophys.* **2002**, *40*, 1002. [[CrossRef](#)]
42. Huang, J.; Ge, J.; Weng, F. Detection of Asia Dust Storms Using Multisensor Satellite Measurements. *Remote Sens. Environ.* **2007**, *110*, 186–191. [[CrossRef](#)]
43. Shimizu, A. Coauthors. Continuous observations of Asian dust and other aerosols by polarization LiDARs in China and Japan during ACE-Asia. *J. Geophys. Res.* **2004**, *109*, D19S17. [[CrossRef](#)]
44. Sugimoto, N.; Shimizu, A.; Matsui, I.; Uno, I.; Arao, K.; Dong, X.; Zhao, S.; Zhou, J.; Lee, C.H. Study of Asian Dust Phenomena in 2001–2003 Using a Network of Continuously Operated Polarization LiDARs. *Water Air Soil Pollut. Focus* **2005**, *5*, 145–157. [[CrossRef](#)]
45. Sugimoto, N.; Hara, Y.; Shimizu, A.; Yumimoto, K.; Uno, I.; Nishikawa, M. Comparison of Surface Observations and a Regional Dust Transport Model Assimilated with LiDAR Network Data in Asian Dust Event of March 29 to April 2. *SOLA* **2007**, *7A*, 13–16. [[CrossRef](#)]
46. Sun, J.; Zhang, M.; Liu, T. Spatial and temporal characteristics of dust storms in China and its surrounding regions, 1960–1999: Relations to source area and climate. *J. Geophys. Res.* **2001**, *106*, 10325–10333. [[CrossRef](#)]
47. Sun, L.; Zhou, X.; Lu, J.; Kim, Y.-P.; Chung, Y.-S. Climatology, trend analysis and prediction of sandstorm and their associated dust fall in China. *Water Air Soil Pollut. Focus* **2003**, *3*, 41–50. [[CrossRef](#)]
48. Chung, Y.S.; Kim, H.S.; Natsagdorj, L.; Jugder, D.; Chang, S.J. On yellow sand occurred during 1997–2000. *J. Meteorol. Soc.* **2004**, *4*, 305–316.
49. Mikhaylov, Y.P. National Atlas of Mongolia. *Mapp. Sc. Remote Sens.* **1993**, *30*, 338–340. [[CrossRef](#)]
50. *International Cloud Atlas, Manual on the Observation of Clouds and Other Meteors*; World Meteorological Organization: Geneva, Switzerland, 1975; Volume 1, WMO No. 407.
51. Available online: <https://namem.gov.mn/eng/> (accessed on 5 January 2019).
52. Available online: <http://www.bjmemc.com.cn/> (accessed on 5 January 2019).
53. Available online: <http://www.kma.go.kr/eng/index.jsp> (accessed on 5 January 2019).
54. Available online: <https://www.nies.go.jp/index-e.html> (accessed on 5 January 2019).

55. Nishikawa, M.; Matsui, I.; Batdorj, D.; Jugder, D.; Mori, I.; Shimizu, A.; Sugimoto, N.; Takahashi, K. Chemical composition of urban airborne particulate matter in Ulaanbaatar. *Atmos/ Environ.* **2011**, *45*, 5710–5715.
56. Sugimoto, N.; Hara, Y.; Shimizu, A.; Nishizawa, T.; Matsui, I.; Nishikawa, M. Analysis of Dust Events in 2008 and 2009 Using the Lidar Network, Surface Observations and the CFORS Model. *Asia-Pacific J. Atmos. Sci.* **2013**, *49*, 27–39. [[CrossRef](#)]
57. Sugimoto, N.I.; Matsui, A.; Shimizu, T.; Nishizawa, Y.; Hara, C.; Xie, I.; Uno, K.; Yumimoto, Z.W.; Yoon, S.C. LiDAR network observations of tropospheric aerosols. *Proc. SPIE* **2008**, *7153*, 71530A. [[CrossRef](#)]
58. Dee, D.P.; Uppala, S.M.; Simmons, A.J.; Berrisford, P.; Poli, P.; Kobayashi, S.; Andrae, U.; Balmaseda, M.A.; Balsamo, G.; Bauer, D.P.; et al. The ERA-Interim Reanalysis: Configuration and Performance of the Data Assimilation system. *Q. J. R. Meteorol. Soc.* **2011**, *137*, 553–597. [[CrossRef](#)]
59. Draxler, R.R.; Rolph, G.D. HYSPLIT (HYbrid Single-Particle Lagrangian Integrated Trajectory) Model Access via NOAA ARL Ready Website. NOAA Air Resources Laboratory. 2003. Available online: <http://ready.arl.noaa.gov/HYSPLIT.php> (accessed on 2 February 2019).
60. Mongolia Second Assessment Report on Climate Change (MARCC). *Ministry of Environment, Nature and Tourism, Mongolia*; MARCC: Ulaanbaatar, China, 2014.
61. Sugimoto, N.; Nishizawa, T.; Shimizu, A.; Matsui, I. Assurance of Data Quality of Aerosol LiDARs and a Method for Obtaining Consistency of Observations with Different Types of LiDARs. *Eerozoru Kenkyu* **2014**, *29*, 166–173.
62. Sugimoto, N.; Shimizu, A.; Matsui, I.; Nishizawa, T. A method for estimating the fraction of mineral dust in particulate matter using PM<sub>2.5</sub>-to-PM<sub>10</sub> ratios. *Particuology* **2016**, *29*, 114–120. [[CrossRef](#)]
63. Jugder, D.; Shinoda, M. Intensity of a Dust Storm in Mongolia during 29–31 March 2007. *Online J. Sci. Online Lett. Atmos.* **2011**, *7A*, 29–31.
64. Jugder, D.; Sugimoto, N.; Shinoda, M.; Matsui, I.; Nishikawa, M. Dust, biomass burning smoke, and anthropogenic aerosol detected by polarization-sensitive Mie LiDAR measurements in Mongolia. *Int. J. Atmos. Environ.* **2012**, *54*, 231–241. [[CrossRef](#)]



© 2019 by the authors. Licensee MDPI, Basel, Switzerland. This article is an open access article distributed under the terms and conditions of the Creative Commons Attribution (CC BY) license (<http://creativecommons.org/licenses/by/4.0/>).